FUNDAMENTAL THERMAL EMISSION PARAMETERS OF MAIN-BELT ASTEROIDS DERIVED FROM ISO *OBSERVATIONS OF (1) CERES

T.G. Müller[1,2], J.S.V. Lagerros[3],
M. Burgdorf[1], T. Lim[4], P. Morris[5], A. Salama[1], B. Schulz[1], and B. Vandenbussche[6]
[1]ISO Data Centre, ESA Astrophysics Division, Villafranca del Castillo, Spain;
[2]MPI für Astronomie, Heidelberg, Germany; [3]Astronomiska observatoriet,
Uppsala, Sweden; [4]Queen Mary and Westfield College, Londen, UK;
[5]SRON, Utrecht, Netherlands; [6]Institute of Astronomy, K.U.Leuven, Belgium

ABSTRACT

In support for the ISO Mission it has been necessary to establish a set of asteroids as photometric standards for the photometric calibration of the instruments (Müller & Lagerros 1998). The new standards are described as rotating ellipsoids. Illumination geometry, heat transfer due to non-zero thermal inertia and surface structure/porosity are taken into account. The characteristic properties of this new thermophysical model (TPM) can be found in Lagerros (1996); Lagerros (1997); Lagerros (1998). Here we apply the TPM to a set of ISO observations on (1) Ceres to derive its thermophysical properties. We determine the thermal inertia, the beaming function, caused by surface roughness and porosity, and the wavelength dependent emissivity. Since we are able to model the full thermal emission over the wavelengths range from 5 to 200μm, we believe that our findings represent fundamental thermal emission properties not only of (1) Ceres, but also of other Main-Belt asteroids.

Key words: ISO; Infrared Astronomy; Asteroids; Ceres; Thermal Emission.

1. INTRODUCTION

Some 30 years ago, with the availability of infrared detectors, it was for the first time possible to measure the thermal emission of asteroids. In parallel with the first observations a model to describe their thermal emission developed, which was mainly based on N-band photometry (Lebofsky et at. 1986 and references therein). It describes asteroids as non-rotating spherical objects in instantaneous equilibrium with the solar insolation. Two empirical correction parameters, the beaming parameter η and the phase angle correction β, are used in order to obtain agreement with the observations. The limitations of the model clearly showed up in the interpretation of IRAS observations (Spencer et at. 1989) and recently in matching KAO measurements (Cohen et at. 1998). The new TPM is based on physical and thermal properties of asteroids and describes the thermal emission without any artificial correction factors. The physical properties, like size, shape and rotational behaviour, are well known for Ceres, but little is known about its thermophysical properties.

We present in Section 2. our ISO observations, taken with 3 different instruments. In Section 3. we briefly describe the Thermophysical Model (TPM), which we used to combine all measurements and to derive emission parameters for Ceres. In Section 4. we show the excellent agreement between model prediction and all observations and discuss the implications for other Main-belt asteroids.

*ISO is an ESA project with instruments funded by ESA Member States (especially the PI countries: France, Germany, the Netherlands and the United Kingdom) and with the participation of ISAS and NASA.

2. OBSERVATIONS

(1) Ceres has been observed many times with ISO, either within dedicated scientific programs or in special calibration measurements. The observing epochs of all data are summarized in Table 1.

2.1. ISOSWS Observations

The SWS observations are taken from a scientific program by A. Salama. On Oct., 30th 1997 a 2.3 h SWS06 grating scan (Graauw et at. 1996) has been performed with 1 up- and 1 down-scan per band. This lead to a full spectrum from 2.38 to 45.2 μm with a spectral resolution ranging from 1000 to 2000. Satellite tracking on Ceres was done with a 2 $arcsec$ stepsize raster. The SWS AOT6 data were processed with the standard product generation pipeline steps. After correction for the solar system tracking steps the final spectrum was obtained by sigma-clipping the data over bins with resolution 500 (σ=3) and rebinning to the same resolution. The photometric calibration of the Ceres spectrum is mainly based on stellar spectra (Schaeidt et at. 1996). At the longwavelength band 4 also Uranus and Neptune (A. Salama,

UT		start	end	AOT	Product
SWS Spectrum					
1997	Oct	30.27	30.37	SWS06	2.38...45.2 μm
LWS Spectrum					
1997	Dec	03.13	03.22	LWS01	43.0...196.9 μm
LWS Photometry					
1996	Feb	18.18	18.19	LWS02	fixed grating
1996	Mar	01.22	01.23	LWS02	position,
1996	Mar	15.11	15.12	LWS02	narrow band
1996	Mar	22.08	22.09	LWS02	photometry at
1996	Jul	31.77	31.78	LWS02	46.1, 56.2,
1996	Aug	07.75	07.76	LWS02	66.1, 75.7,
1996	Oct	02.60	02.61	LWS02	84.8, 102.5,
1997	May	07.46	07.47	LWS02	122.2, 141.8,
1997	Jun	17.37	17.38	LWS02	160.6 and
1997	Jul	02.23	02.24	LWS02	178.0 μm
1997	Dec	03.12	03.13	LWS02	
PHT Photometry					
1996	Aug	18.12	18.19	PHT99	C200 broad band
1996	Mar	07.37	07.41	PHT99	photometry at
1997	Jun	17.26	17.32	PHT99	120.0, 150.0, 170.0,
1997	Jul	02.25	02.28	PHT99	180.0 and 200.0 μm

Table 1. Summary of the ISO observations on Ceres.

priv. comm.) are used for calibration. The absolute accuracy of the spectrum is given with 5...12 % at wavelength below 25 μm and larger than 15 % at longer wavelength (Salama et at. 1997). Figure 1 shows the rebinned SWS spectrum (smooth line), which was used for the later determination of the model parameters, and part of the measured spectrum on top. The transition between reflected light and thermal emission lies in the range 3 to 4 μm, the maximum of the thermal spectrum at 20 to 25 μm.

Figure 1. ISOSWS observations on Ceres, including part of the reflected light and the main part of the thermal emission.

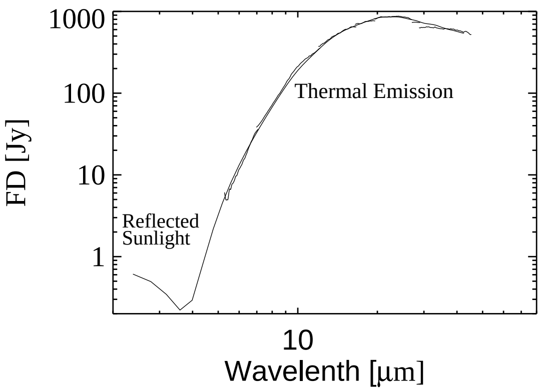

2.2. ISOLWS Observations

(1) Ceres has been observed many times thoughout the whole mission, mainly in LWS02 fixed grating position mode (Clegg et at. 1996). Here we included 11 LWS02 sets, each with 10 narrow band photometric data points taken simultaneously with typically 5-10 min integration time on source. The key wavelengths in fixed grating rest position are 46.1, 56.2, 66.1, 75.7, 84.8, 102.5, 122.2, 141.8, 160.6 and 178.0 μm (with slight changes for a few measurements). Additionally we added one LWS01 full grating scan (scanned only in one direction) ranging from 43.0 to 196.9 μm with a spectral resolution between 150 and 330. The data processing of the LWS observations started with Auto Analysis products on which manual deglitching was performed. Several detectors showed a slow rise of signal during the observations in photometric mode. In these cases only the last part of the integration time was used to determine the flux. The calibration is based on an Uranus model (Griffin et at. 1993). The overall uncertainty lies between 10 and 20 % (Swinyard et at. 1998). It depends on the flux and wavelength range, with higher uncertainties at the longest wavelength where dark current and straylight are sometimes noticeable. For fluxes significantly below 50 Jy at 120 μm an absolute flux accuracy of 50 % is stated (LWS internal report, 1998). Technical problems affected the long wavelengths part (LW 2 to LW 4) of the full grating scan (T. Lim, priv. comm.), therefore we excluded this part in the modelling process.

2.3. ISOPHOT Observations

The PHT data are taken at 4 different epochs with the C200-Camera in a special observing mode (P99), using the Calibration Uplink System (CUS). Each observation consists of 2 internal reference measurements (FCS) and a 4x4 raster on source with the source centered in each pixel for 2-4 min. The key wavelengths are 120.0, 150.0, 170.0, 180.0 and 200.0 μm. The data have been processed partly with ISOPHOT Interactive Analysis (PIA[1]) V7.1 and partly manually outside PIA. The standard data reduction included linear ramp fitting, deglitching on ramp and signal level, reset interval correction and orbit dependent dark signal subtraction (Gabriel et at. 1997a; Gabriel et at. 1997b). The calibration is based exclusively on the planets Uranus and Neptune and on a set of bright standard stars. All calibration standards have been measured in exactly the same observing mode, which enabled us to calibrate each of the 4 detector pixels individually and independently. With off-source observations taken into account we reach a absolute accuracy of 5 to 10 %.

3. THERMOPHYSICAL MODEL

In order to combine all observations to be able to derive and interpret the thermophysical properties, we use a model described in Lagerros (1996); Lagerros (1997); Lagerros (1998) and Müller & Lagerros (1998). The shape of Ceres is approximated by an rotating ellipsoid. The surface temperature is calculated from the energy balance between absorbed solar radiation, thermal emission, and heat conduction into the regolith. The disk integrated model flux

[1]PIA is a joint development by the ESA Astrophysics Division and the ISOPHOT consortium.

at the wavelength λ is

$$F_\lambda = \frac{1}{\pi\Delta^2} \oint_S \epsilon_d B_\lambda(\gamma T)\mu \, dS, \qquad (1)$$

where Δ is the distance to the observer, B_λ the Planck function, and the direction cosine μ projects the surface element dS towards the observer. The "beaming function" γ, and the wavelength- and direction-dependent emissivity ϵ_d are discussed in Müller & Lagerros (1998) and have to be determined from observations.

The size and shape of Ceres (see Table 2) have been determined from occultation observations combined with high resolution measurements and extensive photoelectric photometry (Millis et at. 1987; Saint-Pé et at. 1993).

$2a$	959.2	major ellipsoid axis [km]
a/b	1.00	ellipsoid axis ratio
b/c	1.06	ellipsoid axis ratio
P_{sid}	0.378091	rotation period [$days$]
λ_p,β_p	332,+70	spin vector [°]
γ_o	86	rotation phase [°]
JD_o	2440587.5	zero point in time

Table 2. Shape, size and spin vector for Ceres, as used in the thermophysical model.

The thermal part of the modelling of asteroids can be split up into 2 sections:

- **Reflected Light:** It is described by the geometric albedo p_v, the slope parameter G and the absolute magnitude H. All 3 values are determined from optical measurements for each object individually. We took $H = 3.28\,mag$ and $G = 0.05$ from Lagerkvist et at. (1992) and derived the geometric albedo to $p_v = 0.104$ (Müller & Lagerros 1998).
- **Thermal Emission:** the thermal behaviour is modeled by the beaming parameters ρ and f, the thermal inertia Γ and the hemispherical emissivity $\epsilon_h(\lambda)$. They are reflecting the nature of the asteroid material in a given environment and are derived from the ISO observations. These values can be transfered to other asteroids under certain restrictions.

4. RESULTS AND DISCUSSION

The results we present here are based on a method described in Müller & Lagerros (1998). We took the shape, size and spin vector and also the description of the reflected light as constant input values for the TPM. The approach is then to use various statistical methods on all observations to derive the thermophysical parameters for Ceres. For a given set of parameters the model predicts a flux $F_{\rm m,i}$, which should be compared to the observed flux $F_{\rm o,i}$. This is used as a statistical measure to compare the observations with the model. Ideally one would optimise all model parameters simultaneously to achieve the best possible fit, but this would be a very time consuming and complex process. The approach here is to optimise the parameters separately, and then iterate between the steps to obtain a global solution.
We started with the thermal inertia and beaming. The model parameters Γ, ρ, and f are varied over a three dimensional grid in search for the least-square solution. For a derived solution, the mean and standard deviation of the model ratios r_i are also computed as a consistency check. In a second step the emissivity is determined as function dependent on wavelength, to be fitted to the data. Given the scatter between the dataset, which is in many cases larger than the individual errors, it is not advisable to fit a detailed emissivity model to all specific wavelengths in the database. To improve the statistics the data is divided into a small number of wavelength bins. The weighted mean of observed emissivities is computed for each bin, and is attributed to the mean wavelength $\langle\lambda_i\rangle$ of that bin (Müller 1998). A cubic interpolation is then used to derive a smooth curve connecting these points in the wavelength – emissivity diagram.
Based on this set of ISO observations we find a thermal inertia of $\Gamma = 15\,\mathrm{J\,m^{-2}\,s^{-0.5}\,K^{-1}}$. This value is much smaller than the lunar value of $50\,\mathrm{J\,m^{-2}\,s^{-0.5}\,K^{-1}}$ (Spencer et at. 1989). We believe that this is mainly due to the different environment of the asteroid regolith (lower temperature, lower density) as compared with the lunar evironment. The thermal IR beaming model parameters have been determined to:

$f = 0.6$	fraction of surface covered by craters
$\rho = 0.7$	r.m.s. of the surface slopes

These values are significantly lower than the ones we found from calculations based mainly on ground-based N-band photometry (Müller & Lagerros 1998), but agree well with theoretical considerations (Lagerros 1998).

We got the best solution for the wavelength dependent emissivity by using a cubic interpolation for the emissivity values given in Table 3.

λ [μm]	10.0	20.0	50.0	100	200	400
$\epsilon_d(\lambda)$	0.92	1.00	0.96	0.90	0.83	0.80

Table 3. The hemispherical emissivity $\epsilon_d(\lambda)$ of (1) Ceres in the wavelength range $\lambda = 10$–$400\,\mu$m.

It means that Ceres emitts perfectly at the peak of the thermal emission at around $20\,\mu$m and with a significantly lower efficiency at longer wavelength. Redman et at. (1992) and recently Redman et at. (1998) calculated for several asteroids, including Ceres, a lower Rayleigh-Jeans temperature at submillimetre wavelength compared to the mid-IR or to the centimeter region. They suggest that this is an indication for the presence of a dusty, porous regolith. Scattering processes by grains within the regolith reduce the emissivity in a wavelength dependent fashion. Here we follow this idea, although the interpretation of the results in terms of grain size distribution, regolith structure and material is still on going.

The full thermophysical treatment of Ceres allows us to understand its thermal behaviour and to explain the ISO observations.

Figure 2. Ratio of ISOSWS observations to thermophysical model (TPM) prediction over wavelength. The numbers in the upper part of the diagramm indicate the total flux level.

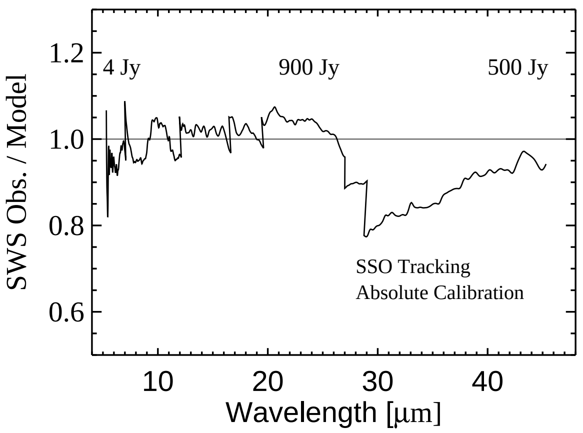

Figure 2 shows the ratio between SWS observations and our TPM prediction. The thermal emission at wavelength between 2.38...45.2 μm is within 5 % well matched. The two steps at wavelength of 26 and 29 μm are due to not perfectly corrected Solar System Object tracking. The different slop longward of 29 μm can also been seen in other objects with a similar spectrum, like Calisto (H. Feuchtgruber, priv. comm.) and has not been fully understood.

Figure 3. Ratio of ISOLWS and ISOPHOT observations to TPM prediction over wavelength. Diamonds represent the LWS fixed grating (FG) observations, the squares the PHT observations and the dots belong to the LWS full scan.

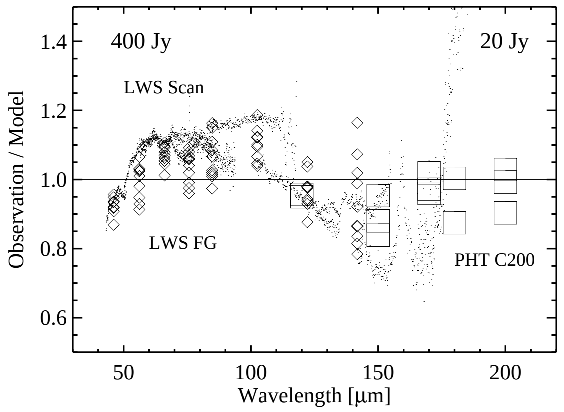

Figure 3 shows the *observation/model*-ratio for the LWS and PHT measurements. The general agreement is in the order of 10 %, although the scatter is much higher. The increase in the LWS scan at the longest wavelength is caused by technical problems during the observations. The general trend in Figure 3 seems to indicate that our emissivity model is not perfect and that the decrease in emissivity beyond 100 μm is even stronger than given in Table 3. The PHT observations confirm our model parameters nicely and emphasize again our finding of emissivities of 0.8 in the FIR, which we used for the model prediction (see Table 3). Again, a trend towards lower emissivity at around 150 μm can be seen.

The excellent agreement on all flux levels over the full thermal emission spectrum of Ceres at different epochs confirm that our values for the thermal properties are well determined. Further preliminary tests of these values on other asteroid observations show that our thermal description of Ceres is also valid for other Main-Belt asteroids. It means that we can model the thermal emission with a high accuracy for all Main-Belt asteroids where the shape and the H-G values are known.

REFERENCES

Clegg, P.E., Ade, P.A.R., Armand, C. et al., A&A, **315L**, 38

Cohen, M., Witteborn, F.C., Roush, T. et al., 1998, AJ, **115**, 1671

Gabriel, C., Acosta–Pulido, J. A., Heinrichsen, I. et al., 1997, Proc. of ADASS VI, 108

Gabriel, C., Schulz, B., Acosta–Pulido, J. A. et al., 1997, Proc. of ADASS VI, 112

De Graauw, T., Haser, L.N., Beintema, D.A. et al., 1996, A&A, **315L**, 49

Griffin, M.J., Orton, G.S., 1993, ICARUS, **105**, 537

Lagerkvist, C.I., Magnusson, P., Williams, I.P. et al., 1992, A&AS, **94**, 43

Lagerros, J.S.V., 1996, A&A, **310**, 1 011

Lagerros, J.S.V., 1997, A&A, **325**, 1 226

Lagerros, J.S.V., 1998, A&A, **332**, 1 123

Lebofsky, L.A., Sykes, M.V., Tedesco, E.F. et al., 1986, ICARUS, **68**, 239

Millis, R.L., Wasserman, L.H., Franz, O.G. et al., 1987, ICARUS, **72**, 507

Müller, T.G., 1997, PhD thesis, Univ. of Heidelberg

Müller, T.G., Lagerros, J.S.V., 1998, A&A, **338**, 340

Redman, R.O., Feldman, P.A., Matthews, H.E., 1998, AJ **116**, 1478

Redman, R.O., Feldman, P.A., Matthews, H.E. et al., 1992, AJ **104**, 405

Salama, A., Feuchtgruber, H., Heras, A. et al., 1997, ESA SP-419, 27

Saint-Pé, O., Combes, M., Rigaut, F., 1993, ICARUS, **105**, 271

Schaeidt, S.G., Morris, P.W., Salama, A. et al., 1996, A&A, **315L**, 55

Spencer, J.R., Lebofsky, L.A., Sykes, M.V., 1989, ICARUS, **78**, 337

Swinyard, B., Clegg, P., Leeks, S. et al., 1998, SPIE **3354**, in press